OPTIMIZATION OF c-Si FILMS FORMED BY ZONE-MELTING RECRYSTALLIZATION FOR THIN-FILM SOLAR CELLS

Thomas Kieliba[1], Johannes Pohl[1], Achim Eyer[1] and Christian Schmiga[2]
[1]Fraunhofer Institute for Solar Energy Systems ISE, Heidenhofstr. 2, 79110 Freiburg, Germany
[2]Institut für Solarenergieforschung Hameln/Emmerthal (ISFH), 31860 Emmerthal, Germany

ABSTRACT

Zone-Melting Recrystallization (ZMR) is able to transform microcrystalline Si films on amorphous substrates into high quality multicrystalline films with grain size comparable to mc-Si ingot material. To reduce the costs of the process a new method to grow the necessary capping oxide directly in the ZMR system has been explored. Further the dependence of crystallographic and electrical film quality on scan speed and film thickness has been investigated. Si film quality has been evaluated by in-situ observation of the solidification front morphology, by Etch Pit Density (EPD) mappings, Modulated Free Carrier Absorption (MFCA) mappings and the preparation of test solar cells. A clear correlation between film properties and solar cell parameters was found. Hydrogen passivation is capable to improve the quality of the Si films significantly. From films grown at low scan speed up to 13.5% efficient thin-film solar cells were fabricated.

1. INTRODUCTION

Crystalline Si thin-film solar cells combine the cost reduction potential of thin-film technologies with the potential to reach high efficiencies. If the substrate material does not restrict process temperatures high Si deposition rates can be achieved and the microcrystalline films can be transformed into a coarse grained structure by ZMR. This way conversion efficiencies comparable to Si solar cells from ingot material have been demonstrated by Mitsubishi Electric Corp. [1].

At Fraunhofer ISE we focus on the use of low-cost ceramic or Si ribbon substrates [2-4]. Using these materials compromises regarding surface flatness and roughness have to be made. With the premise that the Si films have to be thicker than the maximum roughness very thin Si seeding films as used in [5] cancel out. Films suitable for our purpose must have a minimum thickness of a few microns.

ZMR is a key technology for the concept pursued. Defects generated during the ZMR process in the Si seeding film will induce further defects when the film is thickened by epitaxy. Characteristic are subboundaries which manifest in stripes with very high dislocation density in the epitaxial Si film. The overall defect density is mainly determined by two characteristics of the ZMR seeding film growth: First, on the stability of the solidification front which ideally consists of regular cells bounded by (111) facets. Second, on the size of the growth cells determining subboundary spacing.

For the costs of the process the scan speed is the most crucial parameter. Therefore we investigate the effect of scan speed on film quality for different film thickness.

Another cost sensitive aspect is the capping layer deposition. This step is necessary to prevent the agglomeration (*balling-up*) of the molten Si during recrystallization. Growing a thermal oxide directly in the ZMR system simplifies the process.

2. EXPERIMENTAL

2.1 Sample Preparation

For our studies we used Si wafers coated with SiO_2 as insulating model substrates. Most of the experiments were performed on 650–700 µm thick Cz-Si wafers covered with a 1 µm thick thermal oxide. On these wafers either 2 or 8 µm Si were deposited. These seeding films consisted of 0.5 µm undoped Si deposited by Low Pressure Chemical Vapor Deposition (LPCVD) and 1.5 µm or 7.5 µm highly doped (10^{19} cm^{-3}) Si deposited by Atmospheric Pressure CVD (APCVD). For the investigations related to the capping oxide discussed in Section 3.1 in addition 700–800 µm thick damage etched mc-Si wafers covered with 2 µm of SiO_2 deposited by Plasma Enhanced CVD (PECVD) were used. For these samples the seeding films consisted of approximately 8 µm highly doped (approx. 4×10^{18} cm^{-3}) Si deposited by APCVD.

As capping either 2 µm PECVD SiO_2 were deposited or the SiO_2 film was grown directly in the ZMR system. In a pure oxygen atmosphere and a temperature of 1300–1350°C in 15 min an oxide thickness of approximately 150 nm was reached.

Our ZMR system is equipped with CCD cameras for *in-situ* observation of the solidification front morphology [6]. In addition the width of the molten zone is detected by image analysis and used to control the power of the focussed lamp. This way the width of the molten zone can be kept constant within ±5% from the desired value. For these investigations the width was set to values in the range 1–1.5 mm. After ZMR the capping was removed with HF and the seeding films were thickened with 30 µm Si by APCVD epitaxy with a doping concentration of 8×10^{16} cm^{-3}.

For characterization test solar cells of 1 cm^2 area and a simple structure were prepared. The emitter was diffused from a $POCl_3$ source targeting a sheet resistivity of 80 Ω/□. The emitter contacts were defined by photolithography. Since the intermediate oxide disables the contacting of the base from the back side a trench was etched around the active cell area in which an aluminum frame was evaporated.

2.2 Characterization

The crystallographic quality of the films was evaluated at Secco etched surface sections. To account for the inhomogeneous distribution of dislocations we implemented a new setup which is capable of spatially resolved automatic etch pitch counting. By image analysis the density of single etch pits and clusters is counted in an area of 50 x 50 µm. Scanning the sample with a motorized stage a mapping is produced.

To get spatial information on the electrical quality MFCA mappings were measured. The full width at half maximum of the detection spot was approximately 60 µm and the samples were scanned with 25 µm steps. Before the MFCA measurements the Si films were coated with a surface passivating PECVD SiN_x layer.

3. RESULTS

3.1 Effect of Capping Layer Properties

Restricting to comparable process times thermally grown oxides are much thinner than those deposited by PECVD. However our investigations showed that even a 50 nm thin oxide grown in the ZMR system is able to prevent agglomeration of the molten Si. For the experiments discussed below a typical oxide thickness of 150 nm was used. We found that seeding films grown with these thin capping oxides differ from those grown with a 2 µm thick PECVD capping oxide with regard to (i) surface flatness and (ii) subboundary spacing.

(i) Si films grown on thermal oxides are characterized by a faceted surface revealing the individual subgrains as shown in Fig. 1 whereas Si films grown with PECVD oxide capping have a flat surface. This observation was also described by Geis et al. [7].

(ii) The average subboundary spacing of the films grown with thermal oxide is higher than of the films with PECVD capping. With the thinner oxide the same width of the molten zone was reached with less power of the focussed lamp. This fact can be explained with a lower reflectivity in the wavelength of interest. Numerical simulations by Wong et al. [8] predict this behavior. Assuming the model of radiative supercooling [9] a lower reflectivity could increase the difference in power absorption between molten and solidified Si. This effect would increase the depth of the supercooled region and therefore subboundary spacing. The higher average subboundary spacing manifests in a better crystallographic and electrical quality of the films and in better solar cell results as shown in Table I.

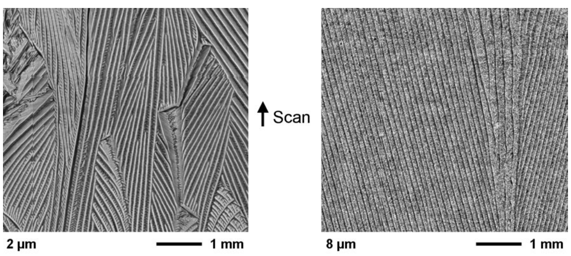

Fig. 1. Optical surface micrographs of Si films with a thickness of 2 and 8 µm after the ZMR process. Both samples were recrystallized at a scan speed of 10 mm/min.

Table I. Electrical parameters of solar cells from samples prepared with different capping types. Except for the combination Cz-Si substrate / PECVD oxide capping, the values are the average of two identically processed cells. The cells have no surface texture, no ARC and are not passivated.

	V_{oc} [mV]	I_{sc} [mA/cm^2]	FF [%]	η [%]
Substrate: Cz-Si				
PECVD oxide	523	15.5	64.5	5.2
Therm. oxide	573	16.0	76.3	7.0
Substrate: mc-Si				
PECVD oxide	531	14.9	64.9	5.2
Therm. oxide	552	16.5	65.7	6.0

3.2 Effect of Scan Speed and Seeding Film Thickness

Si films grown at different scan speeds were analyzed after epitaxy by etch pit density as well as MFCA mappings. For these experiments only the thermal capping oxide was used. In Fig. 2 an etch pit density mapping showing the spatial distribution of dislocations is opposed a MFCA lifetime mapping from the same area. Comparing the lifetimes measured by MFCA with values obtained from IQE measurements and PC1D simulations the absolute values are too high. The reason might be carrier trapping since the injection is changed within a wide range during the measurement.

However a good spatial correlation between lifetime and dislocation density is found. Stripes with high dislocation densities in the region of subboundaries are well reproduced in the MFCA mapping as stripes with low lifetimes.

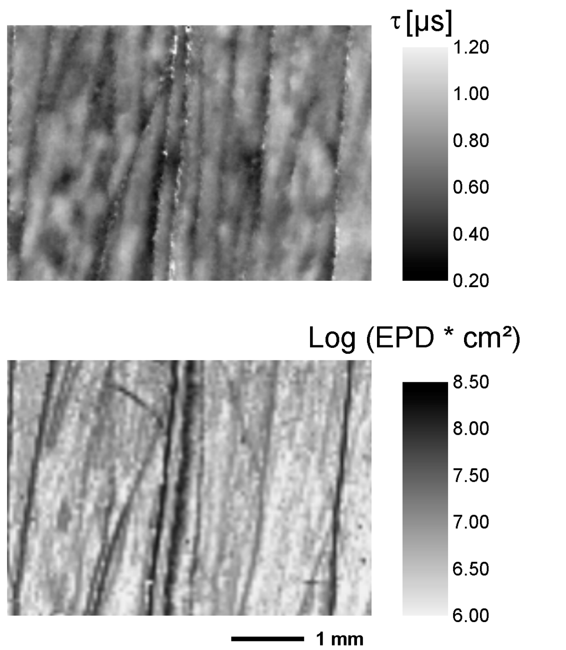

Fig. 2. Comparison of carrier lifetime τ measured by MFCA with etch pit density (EPD). The 8 µm Si seeding film was recrystallized at a scan speed of 10 mm/min.

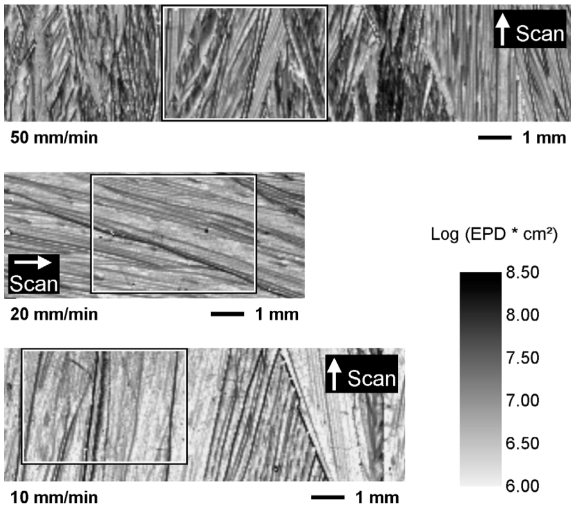

Fig. 3. Etch pit density mappings of ZMR seeding films thickened by epitaxy. The 8 µm thick seeding films were recrystallized at scan speeds of 10, 20 and 50 mm/min respectively. Marked are the areas for which the values are plotted as histograms in Fig. 4.

The etch pit density mappings in Fig. 3 show a significant increase of the average dislocation density with increasing scan speed. As can be determined from the histograms in Fig. 4 an increase of scan speed from 10 to 50 mm/min results approximately in an increase of the average dislocation density from 4×10^6 to 2×10^7 cm^{-2}. The increase in dislocation density correlates well with the decrease in carrier lifetime.

The fact that carrier lifetime is limiting solar cell performance can be seen in Fig. 5 from the dependence of short circuit current density on scan speed. In addition dislocations effect open circuit voltage and fill factor by the limiting current density I_{02}.

For the 2 µm thick films the solar cell parameters are

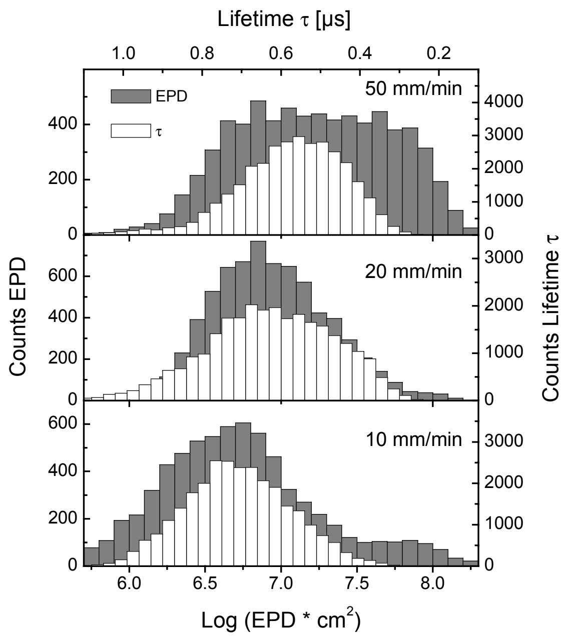

Fig. 4. Histograms of the etch pit density measurements shown in Fig. 3 compared with histograms of MFCA lifetime measurements of the same area.

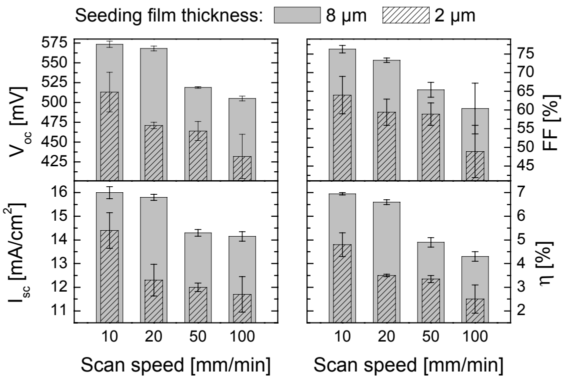

Fig. 5. Dependence of solar cell parameters on scan speed for seeding layer thickness of 8 and of 2 µm. These results are for planar samples without bulk passivation and without ARC.

on a lower level than for the 8 µm thick films. This holds for all scan speeds used. At first sight this contradicts the results of Takami et al. and Naomoto et al. [5,10]. They found that for high scan speeds the defect density of thin films is lower than of thick films. However this might be explained by the different capping types. We observed that for all scan speeds the solidification front was less stable for the 2 µm thick films than for the 8 µm thick films. This behavior is consistent with the run of the subboundaries as shown in Fig. 1. At the 2 µm thick films in most grains the subboundaries are running curved while at the 8 µm thick sample they are running parallel for a long distance.

3.3 Effect of Hydrogen Passivation

Films with different dislocation density were passivated in a remote hydrogen plasma [11] at 350°C for 30 min after metallization. In Table II the results for solar cells processed from different film types are summarized. The three combinations of layer thickness and scan speed correspond to different dislocation densities. Dislocation densities measured at samples grown with the same parameters are given in Table II by their average value ρ_d.

While the absolute improvement in short circuit current density I_{sc} is approximately the same for all three sample types the improvement in open circuit voltage V_{oc} and fill factor *FF* increases with decreasing material quality. This again indicates that dislocations do not only have a substantial effect on the bulk but also on the space charge region and the limiting current density I_{02}. Therefore after hydrogen passivation the relative difference between films processed at high scan speed and those processed at low scan speed is reduced.

From those films recrystallized at low scan speed additional solar cells were fabricated with a more elaborate process. With these solar cells light trapping was realized by surface texturing using alkaline etching. This process takes advantage of the preferential (100) orientation of Si films grown by ZMR. Emitter passivation by oxidation and bulk hydrogen passivation was implemented in the process. Finally the cells were coated with a double layer TiO_2/MgF_2 antireflection coating. Cells fabricated with this process reached an average conversion efficiency of 13.2%. The parameters of the best 1 cm^2 cell on a mc-Si substrate are: $\eta = 13.5\%$, $V_{oc} = 610$ mV, I_{sc} = 30.9

Table II. Solar cell parameters before and after remote plasma hydrogen passivation (RPHP). The values are for planar samples without ARC.

	V_{oc} [mV]	I_{sc} [mA/cm^2]	FF [%]	η [%]
h = 2 µm, v = 20 mm/min, ρ_d = 3.3 x 10^7 cm^{-2}				
Before RPHP	484	12.3	59.0	3.5
After RPHP	534	14.5	62.1	4.8
Improvement	50	2.2	3.1	1.3
h = 8 µm, v = 50 mm/min, ρ_d = 1.6 x 10^7 cm^{-2}				
Before RPHP	530	13.6	67.7	4.9
After RPHP	563	15.9	69.7	6.2
Improvement	33	2.3	2.0	1.3
h = 8 µm, v = 20 mm/min, ρ_d = 8.9 x 10^6 cm^{-2}				
Before RPHP	571	15.5	73.7	6.5
After RPHP	586	17.7	74.0	7.7
Improvement	15	2.2	0.3	1.2

mA/cm² and FF = 71.7. These values were measured at the Fraunhofer ISE calibration laboratory. The relative low fill factor indicates that further technological improvements are possible.

4. SUMMARY

For ZMR a new method to grow the necessary capping oxide has been investigated. Even 150 nm thin oxide layers grown directly in the ZMR system are able to prevent balling-up of the molten Si. With these thin thermal oxides we observed a larger average subboundary spacing than with films grown using our standard PECVD capping oxide. This effect results in lower dislocation density and better solar cell performance.

Using the thermal oxide, film growth was more stable for 8 µm thick Si seeding films than for 2 µm thick ones. This finding is reflected in dislocation density and solar cell performance.

For both film thicknesses a significant decrease of film quality with increasing scan speed was found. However after hydrogen passivation the effect of scan speed is less severe.

From films grown at low scan speed solar cells were fabricated with a process that included surface texture, emitter passivation, hydrogen passivation and double layer antireflection coating. The best of these cells reached an efficiency of 13.5%.

5. ACKNOWLEDGEMENTS

The authors thank S. Riepe for MFCA measurements and the team of the institute’s solar cell department for solar cell processing and measurements. This work was supported by the European Commission in the project SUBARO under contract no. ERK6-CT-1999-00014 and by the German Federal Ministry of Economics and Technology in the project PRISMA under contract no. 0329850C. T. Kieliba is supported by the scholarship program of the German Federal Environmental Foundation.

REFERENCES

[1] H. Morikawa, Y. Nishimoto, H. Naomoto, Y. Kawama, A. Takami, S. Arimoto, T. Ishihara and K. Namba, "16.0 % Efficiency of large area (10 cm x 10 cm) thin film polycrystalline silicon solar cell", Sol. Ener. Mater. Sol. Cells **53**, 23-28 (1998)

[2] T. Kieliba, S. Bau, R. Schober, D. Oßwald, S. Reber, A. Eyer and G. Willeke, "Crystalline silicon thin-film solar cells on $ZrSiO_4$ ceramic substrates", Sol. Ener. Mater. Sol. Cells 74, 261-266 (2002)

[3] A. Eyer, F. Haas, T. Kieliba, D. Oßwald, S. Reber, W. Zimmermann and W. Warta, "Crystalline silicon thin-film (CSiTF) solar cells on SSP and on ceramic substrates", J. Cryst. Growth **225**, 340-347 (2001)

[4] S. Reber, G. Stollwerck, D. Oßwald, T. Kieliba and C. Häßler, "Crystalline silicon thin-film solar cells on silicon nitride ceramics", Proceedings of the 16th European Photovoltaic Solar Energy Conference, (James & James Ltd, London UK 2000) p.1136-1139

[5] H. Naomoto, S. Hamamoto, A. Takami, S. Arimoto and T. Ishihara, "Characterization of thin-film silicon formed by high-speed zone-melting recrystallization process", Sol. Ener. Mater. Sol. Cells 48, 261-267 (1997)

[6] S. Reber, W. Zimmermann, and T. Kieliba, "Zone melting recrystallization of silicon films for crystalline silicon thin-film solar cells", Sol. Ener. Mater. Sol. Cells 65, 409-416 (2001)

[7] M. W. Geis, H. I. Smith, B. Y. Tsaur, J. C. C. Fan, D. J. Silversmith and R. W. Mountain, "Zone-melting recrystallization of Si films with a moveable-strip-heater oven", J. Electrochem. Soc. **129**, 2812-18 (1982)

[8] P. Y. Wong, I. N. Miaoulis, and P. Zavracky, "Optical effects induced by the multilayer nature of SOI films during transient thermal processing with a radiant line heat source", SO Surface Chemistry and Beam-Solid Interactions Symposium, (Mater. Res. Soc 1991) p.445-450

[9] C. P. Grigoropoulos, R. H. Buckholz, and G. A. Domoto, "The role of reflectivity change in optically induced recrystallization of thin silicon films", J. Appl. Phys. 59, 454-458 (1986)

[10] A. Takami, S. Arimoto, H. Naomoto, S. Hamamoto, T. Ishihara, H. Kumabe and T. Murotani, "Thickness dependence of defect density in thin film polycrystalline silicon formed on insulator by zone-melting recrystallization", Proceedings of the 1st World Conference on Photovoltaic Energy Conversion, (IEEE; New York, NY, USA 1994) p.1394-1397

[11] L. Mittelstädt, A. Metz, and R. Hezel, "Hydrogen passivation of defects in EFG ribbon silicon", Sol. Ener. Mater. Sol. Cells **72**, 255-61 (2002)